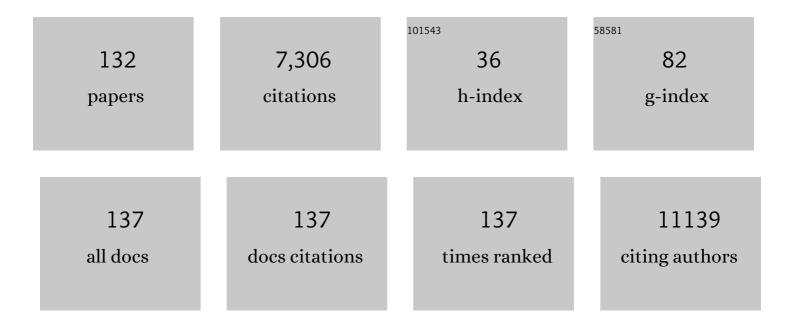
## Urs O Häfeli

List of Publications by Year in descending order

Source: https://exaly.com/author-pdf/7502269/publications.pdf Version: 2024-02-01



<u>Πρς Ο Η</u>Δα<sub>Γ</sub>ιι

#	Article	lF	CITATIONS
1	Metal-ion coordinated self-assembly of human insulin directs kinetics of insulin release as determined by preclinical SPECT/CT imaging. Journal of Controlled Release, 2022, 343, 347-360.	9.9	2
2	SPECT/CT Imaging of <sup>111</sup> Ag for the Preclinical Evaluation of Silver-Based Antimicrobial Nanomedicines. ACS Applied Materials & Interfaces, 2022, 14, 26382-26393.	8.0	5
3	On the consensus nomenclature rules for radiopharmaceutical chemistry – Reconsideration of radiochemical conversion. Nuclear Medicine and Biology, 2021, 93, 19-21.	0.6	43
4	Hybrid Metal–Phenol Nanoparticles with Polydopamine-like Coating for PET/SPECT/CT Imaging. ACS Applied Materials & Interfaces, 2021, 13, 10705-10718.	8.0	22
5	Rapid microwave-based method for the preparation of antimicrobial lignin-capped silver nanoparticles active against multidrug-resistant bacteria. International Journal of Pharmaceutics, 2021, 596, 120299.	5.2	8
6	Preparation of Heat-Denatured Macroaggregated Albumin for Biomedical Applications Using a Microfluidics Platform. ACS Biomaterials Science and Engineering, 2021, 7, 2823-2834.	5.2	1
7	Novel Lignin-Capped Silver Nanoparticles against Multidrug-Resistant Bacteria. ACS Applied Materials & Interfaces, 2021, 13, 22098-22109.	8.0	67
8	Future Advances in Diagnosis and Drug Delivery in Interventional Radiology Using MR Imaging–Steered Theranostic Iron Oxide Nanoparticles. Journal of Vascular and Interventional Radiology, 2021, 32, 1292-1295.e1.	0.5	2
9	Simultaneous SPECT imaging with 123I and 125I - a practical approach to assessing a drug and its carrier at the same time with dual imaging. International Journal of Pharmaceutics, 2021, 606, 120884.	5.2	2
10	Poly(lactide- <i>co</i> -glycolide) Nanoparticles Mediate Sustained Gene Silencing and Improved Biocompatibility of siRNA Delivery Systems in Mouse Lungs after Pulmonary Administration. ACS Applied Materials & Interfaces, 2021, 13, 3722-3737.	8.0	12
11	Navigation of Microrobots by MRI: Impact of Gravitational, Friction and Thrust Forces on Steering Success. Annals of Biomedical Engineering, 2021, 49, 3724-3736.	2.5	7
12	Comparison of Rhenium and Iodine as Contrast Agents in X-Ray Imaging. Contrast Media and Molecular Imaging, 2021, 2021, 1-15.	0.8	6
13	Using in vitro lipolysis and SPECT/CT in vivo imaging to understand oral absorption of fenofibrate from lipid-based drug delivery systems. Journal of Controlled Release, 2020, 317, 375-384.	9.9	10
14	Bioimaging and Biodistribution of the Metalâ€ion ontrolled Selfâ€Assembly of PYY 3–36 Studied by SPECT/CT. ChemBioChem, 2020, 21, 3338-3348.	2.6	5
15	Refinement and validation of infrared thermal imaging (IRT): a non-invasive technique to measure disease activity in a mouse model of rheumatoid arthritis. Arthritis Research and Therapy, 2020, 22, 281.	3.5	14
16	Monosized Polymeric Microspheres Designed for Passive Lung Targeting: Biodistribution and Pharmacokinetics after Intravenous Administration. ACS Nano, 2020, 14, 6693-6706.	14.6	32
17	Quantitative comparison of three widely-used pulmonary administration methods in vivo with radiolabeled inhalable nanoparticles. European Journal of Pharmaceutics and Biopharmaceutics, 2020, 152, 108-115.	4.3	27
18	H2CHXhox: Rigid Cyclohexane-Reinforced Nonmacrocyclic Chelating Ligand for [nat/67/68Ga]Ga3+. Inorganic Chemistry, 2020, 59, 4895-4908.	4.0	15

#	Article	IF	CITATIONS
19	Thiol–Ene Based Polymers as Versatile Materials for Microfluidic Devices for Life Sciences Applications. ACS Applied Materials & Interfaces, 2020, 12, 10080-10095.	8.0	73
20	Magnetic Resonance Navigation for Targeted Embolization in a Two-Level Bifurcation Phantom. Annals of Biomedical Engineering, 2019, 47, 2402-2415.	2.5	26
21	Evaluation of the Tetrakis(3-Hydroxy-4-Pyridinone) Ligand THPN with Zirconium(IV): Thermodynamic Solution Studies, Bifunctionalization, and in Vivo Assessment of Macromolecular 89Zr-THPN-Conjugates. Inorganic Chemistry, 2019, 58, 14667-14681.	4.0	13
22	Precise measurement of intradermal fluid delivery using a low activity technetium-99m pertechnetate tracer. Vaccine, 2019, 37, 7463-7469.	3.8	2
23	Biodegradable magnetic microspheres for drug targeting, temperature controlled drug release, and hyperthermia. Current Directions in Biomedical Engineering, 2019, 5, 161-164.	0.4	11
24	Chloroform compatible, thiol-ene based replica molded micro chemical devices as an alternative to glass microfluidic chips. Lab on A Chip, 2019, 19, 798-806.	6.0	18
25	Radioembolization of Hepatocellular Carcinoma with Built-In Dosimetry: First <i>in vivo</i> Results with Uniformly-Sized, Biodegradable Microspheres Labeled with <sup>188</sup> Re. Theranostics, 2019, 9, 868-883.	10.0	19
26	Temperature controlled camptothecin release from biodegradable magnetic PLGA microspheres. Journal of Magnetism and Magnetic Materials, 2019, 469, 698-703.	2.3	8
27	Selective embolization with magnetized microbeads using magnetic resonance navigation in a controlledâ€flow liver model. Medical Physics, 2019, 46, 789-799.	3.0	16
28	MRI-Compatible Injection System for Magnetic Microparticle Embolization. IEEE Transactions on Biomedical Engineering, 2019, 66, 2331-2340.	4.2	13
29	Microfluidic approaches for the production of monodisperse, superparamagnetic microspheres in the low micrometer size range. Journal of Magnetism and Magnetic Materials, 2019, 471, 286-293.	2.3	10
30	Development of a Coflowing Device for the Size-Controlled Preparation of Magnetic-Polymeric Microspheres as Embolization Agents in Magnetic Resonance Navigation Technology. ACS Biomaterials Science and Engineering, 2018, 4, 1092-1102.	5.2	27
31	Quantitative SPECT imaging and biodistribution point to molecular weight independent tumor uptake for some long-circulating polymer nanocarriers. RSC Advances, 2018, 8, 5586-5595.	3.6	9
32	Design considerations of a hollow microneedle-optofluidic biosensing platform incorporating enzyme-linked assays. Journal of Micromechanics and Microengineering, 2018, 28, 024002.	2.6	20
33	Continuous form-dependent focusing of non-spherical microparticles in a highly diluted suspension with the help of microfluidic spirals. Physics of Fluids, 2018, 30, .	4.0	10
34	Dual-Isotope SPECT/CT Imaging of the Tuberculosis Subunit Vaccine H56/CAF01: Induction of Strong Systemic and Mucosal IgA and T-Cell Responses in Mice Upon Subcutaneous Prime and Intrapulmonary Boost Immunization. Frontiers in Immunology, 2018, 9, 2825.	4.8	23
35	Dual SPECT imaging of <sup>111</sup> In and <sup>67</sup> Ga to simultaneously determine <i>in vivo</i> the pharmacokinetics of different radiopharmaceuticals: a quantitative tool in pre-clinical research. Physics in Medicine and Biology, 2018, 63, 235029.	3.0	6
36	H <sub>4</sub> octox: Versatile Bimodal Octadentate Acyclic Chelating Ligand for Medicinal Inorganic Chemistry. Journal of the American Chemical Society, 2018, 140, 15487-15500.	13.7	32

#	Article	IF	CITATIONS
37	Heterogeneous distribution of trastuzumab in HER2-positive xenografts and metastases: role of the tumor microenvironment. Clinical and Experimental Metastasis, 2018, 35, 691-705.	3.3	38
38	Microfluidic-Based Synthesis of Magnetic Nanoparticles Coupled with Miniaturized NMR for Online Relaxation Studies. Analytical Chemistry, 2018, 90, 9975-9982.	6.5	38
39	A single microfluidic chip with dual surface properties for protein drug delivery. International Journal of Pharmaceutics, 2017, 521, 84-91.	5.2	11
40	188Re image performance assessment using small animal multi-pinhole SPECT/PET/CT system. Physica Medica, 2017, 33, 26-37.	0.7	12
41	Tomographic magnetic particle imaging of cancer targeted nanoparticles. Nanoscale, 2017, 9, 18723-18730.	5.6	107
42	Accuracy of Rhenium-188 SPECT/CT activity quantification for applications in radionuclide therapy using clinical reconstruction methods. Physics in Medicine and Biology, 2017, 62, 6379-6396.	3.0	7
43	A new tetrapodal 3-hydroxy-4-pyridinone ligand for complexation of 89zirconium for positron emission tomography (PET) imaging. Dalton Transactions, 2017, 46, 9654-9663.	3.3	27
44	Facile microwave synthesis of uniform magnetic nanoparticles with minimal sample processing. Journal of Magnetism and Magnetic Materials, 2017, 421, 283-291.	2.3	14
45	Characterization of alendronic- and undecylenic acid coated magnetic nanoparticles for the targeted delivery of rosiglitazone to subcutaneous adipose tissue. Nanomedicine: Nanotechnology, Biology, and Medicine, 2017, 13, 559-568.	3.3	12
46	Metal nanoparticles: understanding the mechanisms behind antibacterial activity. Journal of Nanobiotechnology, 2017, 15, 65.	9.1	1,487
47	Fractionation of Magnetic Microspheres in a Microfluidic Spiral: Interplay between Magnetic and Hydrodynamic Forces. PLoS ONE, 2017, 12, e0169919.	2.5	7
48	Effective Control of Molds Using a Combination of Nanoparticles. PLoS ONE, 2017, 12, e0169940.	2.5	28
49	An Ultra-High Performance Liquid Chromatography-Tandem Mass Spectrometry Method for the Quantification of Vancomycin Requiring Only 2 µL of Rabbit Serum. American Journal of Analytical Chemistry, 2017, 08, 553-563.	0.9	4
50	Development and Validation of an Artificial Mechanical Skin Model for the Study of Interactions between Skin and Microneedles. Macromolecular Materials and Engineering, 2016, 301, 306-314.	3.6	25
51	Accuracy, reproducibility, and uncertainty analysis of thyroidâ€probeâ€based activity measurements for determination of dose calibrator settings. Medical Physics, 2016, 43, 6309-6321.	3.0	4
52	Multiâ€modal magnetic resonance imaging and histology of vascular function in xenografts using macromolecular contrast agent hyperbranched polyglycerol (HPGâ€GdF). Contrast Media and Molecular Imaging, 2016, 11, 77-88.	0.8	9
53	Osteogenic and anti-osteoporotic effects of risedronate-added calcium phosphate silicate cement. Biomedical Materials (Bristol), 2016, 11, 045002.	3.3	23
54	Integrated hollow microneedle-optofluidic biosensor for therapeutic drug monitoring in sub-nanoliter volumes. Scientific Reports, 2016, 6, 29075.	3.3	76

#	Article	IF	CITATIONS
55	A micromechanical comparison of human and porcine skin before and after preservation by freezing for medical device development. Scientific Reports, 2016, 6, 32074.	3.3	113
56	A Comprehensive Study of Osteogenic Calcium Phosphate Silicate Cement: Material Characterization and In Vitro/In Vivo Testing. Advanced Healthcare Materials, 2016, 5, 457-466.	7.6	25
57	Production of monodispersed magnetic polymeric microspheres in a microfluidic chip and 3D simulation. Microfluidics and Nanofluidics, 2016, 20, 1.	2.2	13
58	Simulation and experimental determination of the online separation of blood components with the help of microfluidic cascading spirals. Biomicrofluidics, 2015, 9, 044110.	2.4	15
59	A microneedle-based method for the characterization of diffusion in skin tissue using doxorubicin as a model drug. Biomedical Microdevices, 2015, 17, 9967.	2.8	37
60	Utilization of nanoparticles as Xâ€ray contrast agents for diagnostic imaging applications. Contrast Media and Molecular Imaging, 2015, 10, 81-95.	0.8	65
61	Electrospun magnetic nanofibre mats – A new bondable biomaterial using remotely activated magnetic heating. Journal of Magnetism and Magnetic Materials, 2015, 380, 330-334.	2.3	25
62	Preparation, characterization, release kinetics, and <i>in vitro</i> cytotoxicity of calcium silicate cement as a risedronate delivery system. Journal of Biomedical Materials Research - Part A, 2014, 102, 2295-2304.	4.0	17
63	A Comprehensive Review on the Pharmacokinetics of Antibiotics in Interstitial Fluid Spaces in Humans: Implications on Dosing and Clinical Pharmacokinetic Monitoring. Clinical Pharmacokinetics, 2014, 53, 695-730.	3.5	41
64	Arrays of hollow out-of-plane microneedles made by metal electrodeposition onto solvent cast conductive polymer structures. Journal of Micromechanics and Microengineering, 2013, 23, 085011.	2.6	52
65	Continuously manufactured magnetic polymersomes – a versatile tool (not only) for targeted cancer therapy. Nanoscale, 2013, 5, 11385.	5.6	61
66	Influence of Iron Oxide Nanoparticles on Innate and Genetically Modified Secretion Profiles of Mesenchymal Stem Cells. IEEE Transactions on Magnetics, 2013, 49, 389-393.	2.1	8
67	Uniform polymer microspheres: monodispersity criteria, methods of formation and applications. Nanomedicine, 2013, 8, 265-285.	3.3	44
68	Multifunctional nanocarriers for biomedical applications. , 2013, , .		2
69	Fabrication of hollow microneedle arrays using electrodeposition of metal onto solvent cast conductive polymer structures. , 2013, , .		1
70	A microfluidic chip for size dependent fractionation of magnetic microspheres for magnetic drug targeting. Biomedizinische Technik, 2012, 57, .	0.8	0
71	Focused Magnetic Stem Cell Targeting to the Retina Using Superparamagnetic Iron Oxide Nanoparticles. Cell Transplantation, 2012, 21, 1137-1148.	2.5	123
72	Therapeutic Drug Monitoring in Interstitial Fluid: A Feasibility Study Using a Comprehensive Panel of Drugs. Journal of Pharmaceutical Sciences, 2012, 101, 4642-4652.	3.3	35

#	Article	IF	CITATIONS
73	Nanoprobes for hybrid SPECT/MR molecular imaging. Nanomedicine, 2012, 7, 719-733.	3.3	21
74	A microfluidic spiral for size-dependent fractionation of magnetic microspheres. Journal of Magnetism and Magnetic Materials, 2012, 324, 3791-3798.	2.3	23
75	Development and evaluation of a dual-modality (MRI/SPECT) molecular imaging bioprobe. Nanomedicine: Nanotechnology, Biology, and Medicine, 2012, 8, 1007-1016.	3.3	66
76	Hyperbranched Polyglycerols as Trimodal Imaging Agents: Design, Biocompatibility, and Tumor Uptake. Bioconjugate Chemistry, 2012, 23, 372-381.	3.6	45
77	Long-circulating non-toxic blood pool imaging agent based on hyperbranched polyglycerols. International Journal of Pharmaceutics, 2012, 422, 418-427.	5.2	38
78	Hollow Out-of-Plane Polymer Microneedles Made by Solvent Casting for Transdermal Drug Delivery. Journal of Microelectromechanical Systems, 2012, 21, 44-52.	2.5	36
79	Crucial Ignored Parameters on Nanotoxicology: The Importance of Toxicity Assay Modifications and "Cell Visionâ€+ PLoS ONE, 2012, 7, e29997.	2.5	154
80	One to chelate them all: investigation of a versatile, bifunctional chelator for 64Cu, 99mTc, Re and Co. Dalton Transactions, 2011, 40, 6253.	3.3	19
81	Evaluation of 1111n labeled antibodies for SPECT imaging of mesothelin expressing tumors. Nuclear Medicine and Biology, 2011, 38, 885-896.	0.6	27
82	Radiolabeling of fab and f(ab′)2 antibody fragments with 99mTc(I) tricarbonyl core using a new bifunctional tridentate ligand. Nuclear Medicine Communications, 2011, 32, 324-329.	1.1	9
83	Effects of chemical and physical parameters in the generation of microspheres by hydrodynamic flow focusing. Colloids and Surfaces B: Biointerfaces, 2011, 87, 361-368.	5.0	19
84	Magnetic fluid hyperthermia: Focus on superparamagnetic iron oxide nanoparticles. Advances in Colloid and Interface Science, 2011, 166, 8-23.	14.7	1,125
85	Comparison of vancomycin concentrations in blood and interstitial fluid: a possible model for less invasive therapeutic drug monitoring. Clinical Chemistry and Laboratory Medicine, 2011, 49, 2123-5.	2.3	10
86	A new approach for the in vitro identification of the cytotoxicity of superparamagnetic iron oxide nanoparticles. Colloids and Surfaces B: Biointerfaces, 2010, 75, 300-309.	5.0	264
87	Targeted Delivery of Magnetic Cobalt Nanoparticles to the Eye Following Systemic Administration. AIP Conference Proceedings, 2010, , .	0.4	10
88	Study of the Binding Capacity of Heparin Functionalized Magnetic Microparticles for Cardiac Lipoprotein Lipase and their Preliminary Evaluation Ex Vivo in Rat Hearts. , 2010, , .		1
89	Lung Perfusion Imaging with Monosized Biodegradable Microspheres. Biomacromolecules, 2010, 11, 561-567.	5.4	37
90	In vivo evaluation of a microneedle-based miniature syringe for intradermal drug delivery. Biomedical Microdevices, 2009, 11, 943-950.	2.8	60

#	Article	IF	CITATIONS
91	Preparation of biodegradable magnetic microspheres with poly(lactic acid)-coated magnetite. Journal of Magnetism and Magnetic Materials, 2009, 321, 1356-1363.	2.3	85
92	Magnetic iron particles with high magnetization useful for immunoassay. Journal of Magnetism and Magnetic Materials, 2009, 321, 1676-1678.	2.3	12
93	Radiolabeling of Biodegradable Polymeric Microspheres with [ <sup>99m</sup> Tc(CO) <sub>3</sub> ] <sup>+</sup> and <i>in Vivo</i> Biodistribution Evaluation using MicroSPECT/CT Imaging. Bioconjugate Chemistry, 2009, 20, 1209-1217.	3.6	29
94	Design, Synthesis, and Imaging of Small Amphiphilic Rhenium and <sup>99m</sup> Technetium Tricarbonyl Complexes. Bioconjugate Chemistry, 2009, 20, 1002-1009.	3.6	9
95	Superparamagnetic Iron Oxide Nanoparticles with Rigid Cross-linked Polyethylene Glycol Fumarate Coating for Application in Imaging and Drug Delivery. Journal of Physical Chemistry C, 2009, 113, 8124-8131.	3.1	164
96	Multiphysics Flow Modeling and in Vitro Toxicity of Iron Oxide Nanoparticles Coated with Poly(vinyl) Tj ETQq0 0	0 rgBT /Ον	erlock 10 Tf
97	Cell Uptake and <i>in Vitro</i> Toxicity of Magnetic Nanoparticles Suitable for Drug Delivery. Molecular Pharmaceutics, 2009, 6, 1417-1428.	4.6	242
98	Use of hydrodynamic flow focusing for the generation of biodegradable camptothecinâ€loaded polymer microspheres. Journal of Pharmaceutical Sciences, 2008, 97, 4943-4954.	3.3	23
99	Process and formulation variables in the preparation of injectable and biodegradable magnetic microspheres. Biomagnetic Research and Technology, 2007, 5, 2.	2.0	36
100	Fibrin glue system for adjuvant brachytherapy of brain tumors with 188Re and 186Re-labeled microspheres. European Journal of Pharmaceutics and Biopharmaceutics, 2007, 65, 282-288.	4.3	22
101	One-pot syntheses, coordination, and characterization of application-specific biodegradable ligand-polymers. Dalton Transactions, 2007, , 4439.	3.3	14
102	The biocompatibility and toxicity of magnetic particles. Laboratory Techniques in Biochemistry and Molecular Biology / Edited By T S Work [and] E Work, 2007, , 163-223.	0.2	7
103	Modeling of magnetic bandages for drug targeting: Button vs. Halbach arrays. Journal of Magnetism and Magnetic Materials, 2007, 311, 323-329.	2.3	57
104	â€~Magnetic bandages' for targeted delivery of therapeutic agents. Journal of Physics Condensed Matter, 2006, 18, S2877-S2891.	1.8	35
105	Radiolabelling of poly(histidine) derivatized biodegradable microspheres with the 188Re tricarbonyl complex [188Re(CO)3(H2O)3]+. Nuclear Medicine Communications, 2005, 26, 453-458.	1.1	21
106	Synergistic cytotoxic effects of zoledronic acid and radiation in human prostate cancer and myeloma cell lines. International Journal of Radiation Oncology Biology Physics, 2005, 61, 535-542.	0.8	49
107	Optical method for measurement of magnetophoretic mobility of individual magnetic microspheres in defined magnetic field. Journal of Magnetism and Magnetic Materials, 2005, 293, 224-239.	2.3	52
108	Suppression of Prostate Carcinogenesis by Dietary Supplementation of Celecoxib in Transgenic Adenocarcinoma of the Mouse Prostate Model. Cancer Research, 2004, 64, 3334-3343.	0.9	169

#	Article	IF	CITATIONS
109	Preparation and characterization of radioactive Co/188Re stents intended for lung cancer treatment using an electrodeposition method. Journal of Medical Engineering and Technology, 2004, 28, 197-204.	1.4	13
110	Magnetically modulated therapeutic systems. International Journal of Pharmaceutics, 2004, 277, 19-24.	5.2	232
111	Preparation and radiolabeling of surface-modified magnetic nanoparticles with rhenium-188 for magnetic targeted radiotherapy. Journal of Magnetism and Magnetic Materials, 2004, 277, 165-174.	2.3	141
112	Development of an automated electroplater and dosimetry system for the electrodeposition and quality control of radioactive stents. Applied Radiation and Isotopes, 2004, 61, 1313-1321.	1.5	5
113	Magnetizable needles and wires–modeling an efficient way to target magnetic microspheres in vivo. Biorheology, 2004, 41, 599-612.	0.4	53
114	90Y-oxine-ethiodol, a potential radiopharmaceutical for the treatment of liver cancer. Applied Radiation and Isotopes, 2003, 58, 567-573.	1.5	19
115	Radiolabeling of magnetic targeted carriers (MTC) with indium-111. Nuclear Medicine and Biology, 2003, 30, 761-769.	0.6	12
116	Self-absorption correction for 32P,198Au and 188 Re stents: Dose point kernel calculations versus Monte Carlo. Medical Physics, 2001, 28, 1883-1897.	3.0	4
117	Stability of biodegradable radioactive rhenium (Re-186 and Re-188) microspheres after neutron-activation. Applied Radiation and Isotopes, 2001, 54, 869-879.	1.5	42
118	Novel chelator containing particles specific for controlled radioisotope delivery. Journal of Labelled Compounds and Radiopharmaceuticals, 2001, 44, S838.	1.0	1
119	In response to DRS. Parikh and Nori. International Journal of Radiation Oncology Biology Physics, 2000, 47, 261-263.	0.8	1
120	Local Application of Beta-Particle Radiation to Reduce Venous Anastomotic Intimal Hyperplasia in Polytetrafluoroethylene Arteriovenous Fistulas. Vascular Surgery, 2000, 34, 377-383.	0.3	1
121	Dosimetry of a W-188/Re-188 beta line source for endovascular brachytherapy. Medical Physics, 2000, 27, 668-675.	3.0	14
122	Modeling rhenium-186 and rhenium-188 distribution in a neutron-activated rhenium wire and effect of the distribution on beta dosimetry in a water phantom. Applied Radiation and Isotopes, 1999, 51, 543-549.	1.5	3
123	Hepatic tumor radioembolization in a rat model using radioactive rhenium (186Re/188Re) glass microspheres. International Journal of Radiation Oncology Biology Physics, 1999, 44, 189-199.	0.8	64
124	Parenchymal cell proliferation in coronary arteries after percutaneous transluminal coronary angioplasty: a human tissue bank study. International Journal of Radiation Oncology Biology Physics, 1999, 45, 963-968.	0.8	7
125	In vitro and in vivo toxicity of magnetic microspheres. Journal of Magnetism and Magnetic Materials, 1999, 194, 76-82.	2.3	135
126	Preparation and properties of radioactive rhenium glass microspheres intended forin vivo		37

radioembolization therapy. , 1998, 42, 617-625.

#	Article	IF	CITATIONS
127	Electrodeposition of radioactive rhenium onto stents to prevent restenosis. Biomaterials, 1998, 19, 925-933.	11.4	22
128	Preparation and properties of radioactive rhenium glass microspheres intended for in vivo radioembolization therapy. Journal of Biomedical Materials Research Part B, 1998, 42, 617-625.	3.1	1
129	Magnetically Targeted Microspheres for Intracavitary and Intraspinal Y-90 Radiotherapy. , 1997, , 501-516.		13
130	Analysis of Microspheres in Living Cells by Confocal Microscopy. , 1997, , 149-161.		0
131	Effective targeting of magnetic radioactive90Y-microspheres to tumor cells by an externally applied magnetic field. Preliminary in vitro and in vivo results. Nuclear Medicine and Biology, 1995, 22, 147-155.	0.6	107
132	Magnetically directed poly(lactic acid)90Y-microspheres: Novel agents for targeted intracavitary radiotherapy. Journal of Biomedical Materials Research Part B, 1994, 28, 901-908.	3.1	53